

Supplementary Materials for

Accelerated ex situ breeding of *GBSS*- and *PTST1*-edited cassava for modified starch

Simon E. Bull*, David Seung, Christelle Chanez, Devang Mehta, Joel-Elias Kuon, Elisabeth Truernit, Anton Hochmuth, Irene Zurkirchen, Samuel C. Zeeman, Wilhelm Gruissem, Hervé Vanderschuren*

*Corresponding author. Email: sbull@ethz.ch (S.E.B.); herve.vanderschuren@ulg.ac.be (H.V.)

Published 5 September 2018, *Sci. Adv.* 4, eaat6086 (2018)
DOI: 10.1126/sciadv.aat6086

This PDF file includes:

- Fig. S1. Molecular screening of transgenic plants.
- Fig. S2. Efficacy of the genome editing constructs in vitro and in vivo.
- Fig. S3. Screening of predicted off-target cleavage sites for *GBSSsgRNA4* and *PTSTsgRNA2*.
- Fig. S4. Morphology of glasshouse-cultivated *gbss* and *ptst* lines.
- Fig. S5. CLDs in storage root starch of *gbss* and *ptst* lines.
- Fig. S6. Flow cytometry analysis of starch granule size in *gbss* and *ptst* lines.
- Fig. S7. Scanning electron microscopy of purified *gbss* and *ptst* starch granules.
- Fig. S8. Physicochemical properties of *gbss* and *ptst* starch.

SUPPLEMENTARY MATERIALS

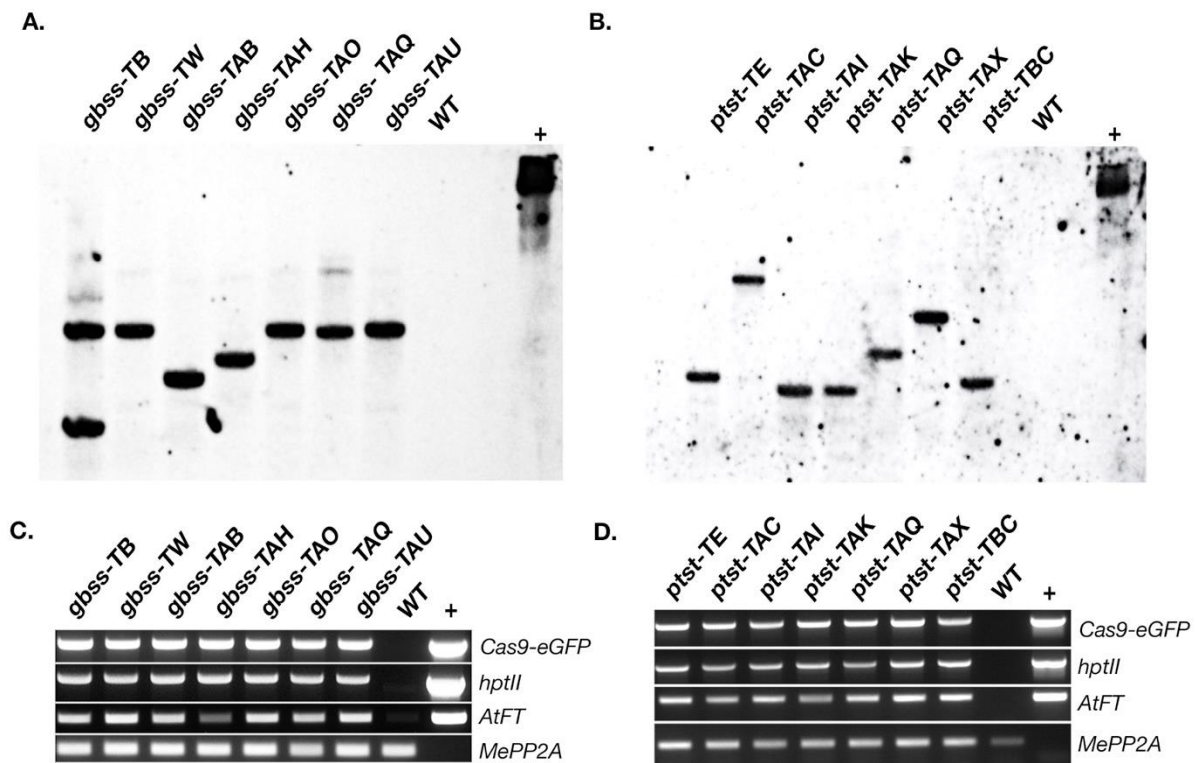


Fig. S1. Molecular screening of transgenic plants. (A) and (B) Southern blotting of genomic DNA fragments from putative plant lines harboring *pCas9-sgGBSS-FT* or *pCas9-sgPTST-FT*, respectively, was followed by hybridization with a DIG-labelled *hptII* probe. WT DNA (negative control) and supercoiled plasmid DNA (*pCas9-sgGBSS-FT* or *pCas9-sgPTST-FT* (positive control; lanes +) are shown. (C) and (D) Products following PCR-amplification of transgenes from genomic DNA from putative plant lines harboring *pCas9-sgGBSS-FT* or *pCas9-sgPTST-FT*, respectively, were resolved by agarose gel electrophoresis. Successful amplification for *Cas9-eGFP*, *hptII* and *AtFT* can be observed in all *gbss* and *ptst* lines. WT DNA (negative control) and plasmid DNA (*pCas9-sgGBSS-FT* or *pCas9-sgPTST-FT*; positive control; lanes +) are shown. Amplification of the endogenous reference gene (*MePP2A*) is also shown.

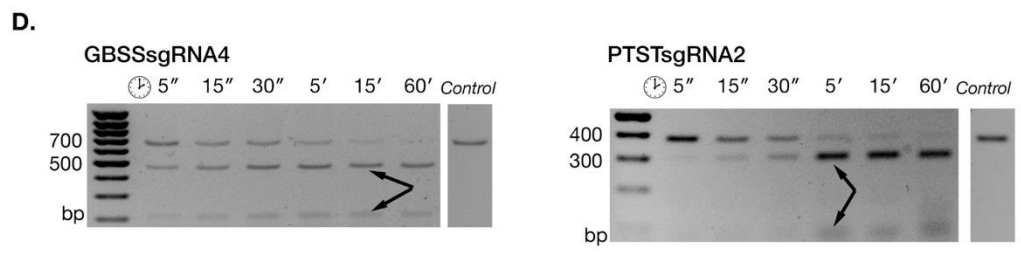
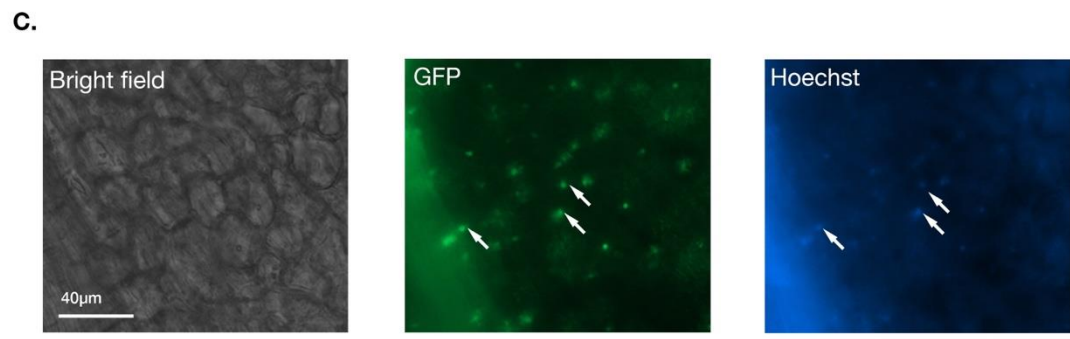
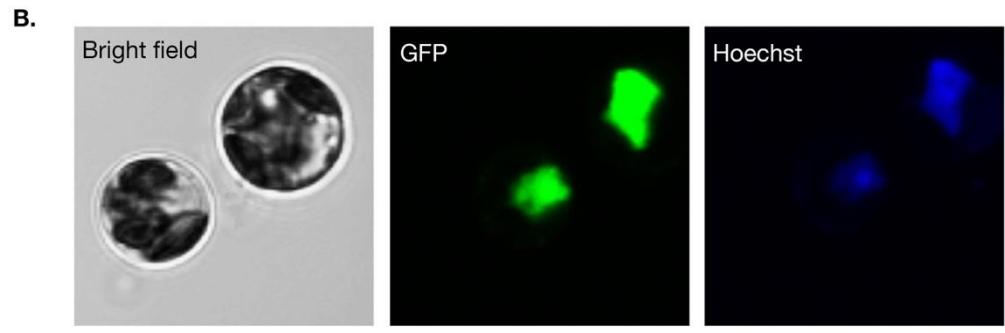
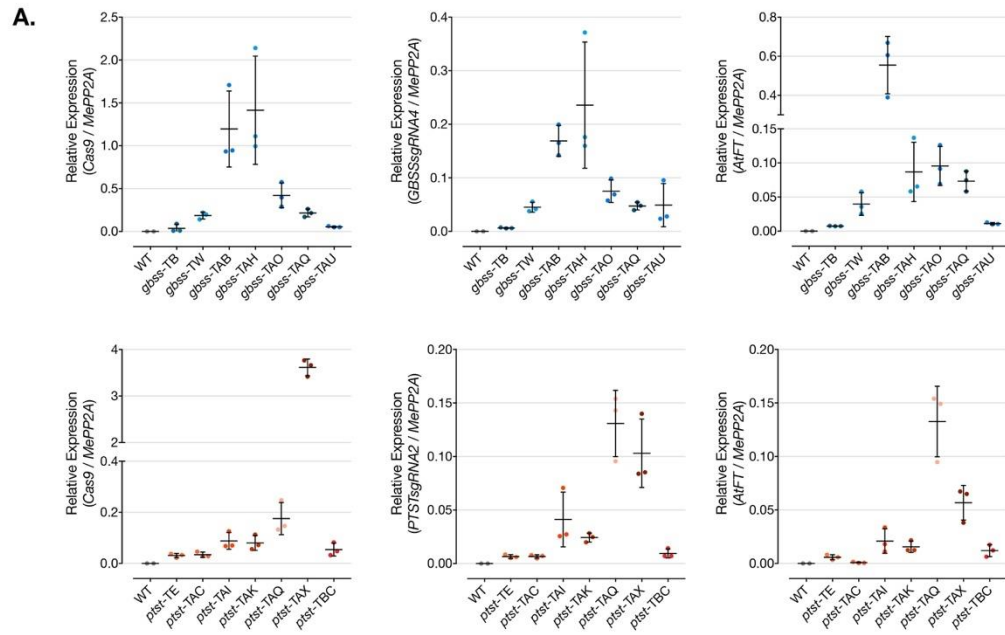


Fig. S2. Efficacy of the genome editing constructs in vitro and in vivo. (A) sqRT-PCR revealing expression of *Cas9*, *GBSSsgRNA₄* or *PTSTsgRNA₂* and *AtFT* relative to the reference gene (*MePP_{2A}*) in *pCas9-sgGBSS-FT* and *pCas9-sgPTST-FT* transformed lines. *n* = 3 plants, except WT *n* = 2 plants, mean ± SD shown. (B) Cassava cv. 60444 leaf protoplasts following transformation with *pCaMV_{35S}-Cas9-eGFP-NLS-tHSP*. eGFP fluorescence and Hoechst stained nuclei. (C) Observation of eGFP fluorescence in regenerating somatic cotyledons after *Agrobacterium*-mediated stable transformation of FEC using the binary construct *pCas9-sgGBSS-FT*. White arrows indicate the position of some nuclei. (D) Ribonucleoprotein complexes with *GBSSsgRNA₄* and *PTSTsgRNA₂* were used to determine cleavage efficiency in the presence of target dsDNA templates *in vitro*. Reaction products were resolved by agarose gel electrophoresis (bp, sizes marked) and cleavage fragments are indicated with arrows. Untreated loading control of *GBSS* and *PTST₁* dsDNA at the 15' time point (control).

A.

	1	10	20	23	Region in genome	Detection Method	Off-Target indels?
GBSSsgRNA4	828 837 850						
	T G C T T G G G A T A C C C T C T G T A T C G G						
Off-target 1	T G C T T A A A A A T C T C T G T A T C G G				Intron. Manes.03G064300.1	Surveyor Assay & Sanger Seq.	No
2	T G C T T A A A A A T C T C T G T A T C G G				Intergenic, non-coding	Surveyor Assay	No
3	C A A T T G G G A G T T C T C T G T A T C G G				Intergenic, non-coding	Surveyor Assay	No
4	T G C T T A G G T A T T C T C T G T A T C G G				Intergenic, non-coding	Surveyor Assay & Sanger Seq.	No
5	T G C T T A G G T A T T C T C T G T A T C G G				Intergenic, non-coding	Surveyor Assay	No
6	G T T G G G A A C C T C T G T A T C G G				Intergenic, non-coding	Surveyor Assay	No
7	G T T G G G A A C C T C T G T A T C G G				Intergenic, non-coding	Surveyor Assay	No
8	T G C T T A G G T A T T C T C T G T A T C G G				Intron. Manes.02G181700.1	Surveyor Assay & Sanger Seq.	No
PTSTsgRNA2	832 841 854						
	G A A T A T C C T A C G G T T G C G A G G G						
Off-target 1	T G A T A T T C T A C G G T T G A T T A G G G				Promoter. Manes.09G127400.1	Sanger Seq.*	No
2	T G A T A T T C T A C G G T T G A T T A G G G				Promoter. Manes.09G127400.1	Sanger Seq.	No
3	T A A T A G T C T A C G G T T G A T T G G				Intron. Manes.06G152600.1	Sanger Seq.	No
4	G A A G A A T T A C A T T T G G A A T G G				Intron/exon. Manes.03G096800.1	Sanger Seq.	No
5	G A A G A A C A C C T T T G G C A T G G				Intergenic, non-coding	Surveyor Assay	No
6	G A A G A T G T A C A T T T G G C A T G G				Intergenic, non-coding	Surveyor Assay	No
7	C A A C A T C C A A C C G T T G G C A G G G				Intergenic, non-coding	Surveyor Assay	No
8	G A A G A A A C A C T T T T G G C A T G G				Intergenic, non-coding	Surveyor Assay	No

B.

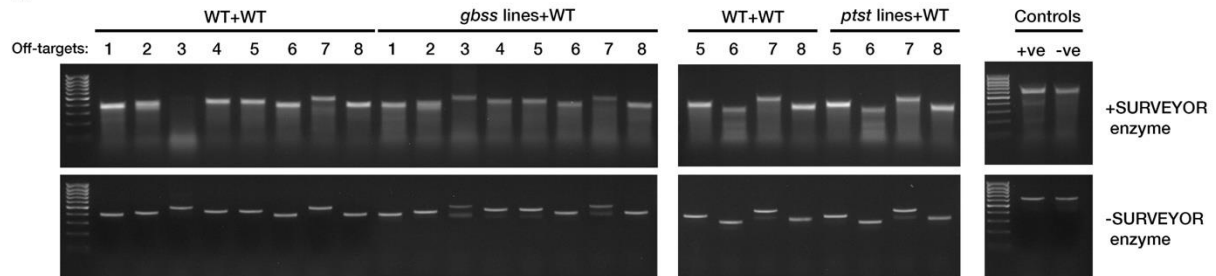


Fig. S3. Screening of predicted off-target cleavage sites for *GBSSsgRNA4* and *PTSTsgRNA2*.

(A) Selected, predicted off-target sites for *GBSSsgRNA4* and *PTSTsgRNA2*. Indels at off-target sites were screened for using the Surveyor® assay and/or Sanger sequencing of the amplified regions. *PTST off-target #1 and #2 represent the two heterozygous haplotypes of the gene containing the off-target sequence and mapped to different scaffolds. Note that in other cases the same off-target sequence was identified in two different genomic locations e.g. *GBSS* off-target #1 and #2. (B) Surveyor® assay of amplicons spanning the off-target sites. Screen for heteroduplexes between WT and *gbss* or *ptst* lines. WT+WT homoduplex and vector controls shown. Experiments with Surveyor® enzyme (upper image) and without (lower image). No indels were detected at any predicted off-target site in any line of *gbss*, *ptst* or WT control.

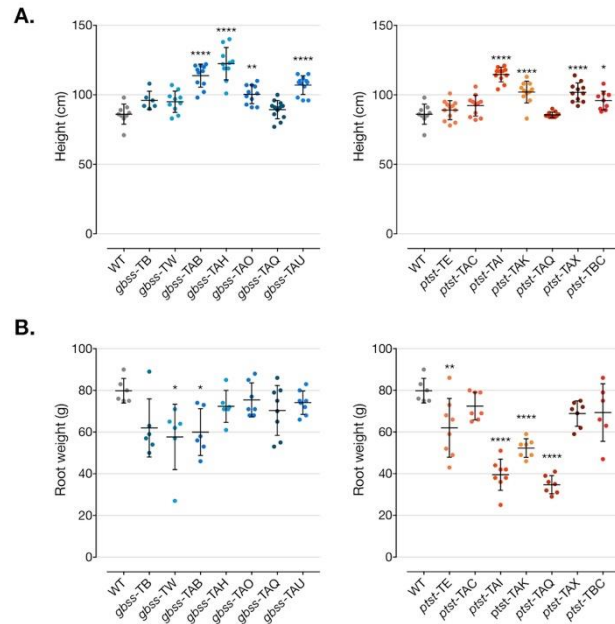


Fig. S4. Morphology of glasshouse-cultivated *gbss* and *ptst* lines. (A) Plant height and (B) total root mass per plant after 6-month growth. WT (negative control) shown. Plant height: $n = 9-12$ plants, except *gbss*-TB, $n = 6$ plants. Root mass: $n = 6-8$ plants. Statistical variation using Tukey's multiple comparisons test ($P < 0.0001=****$, $P < 0.001=***$, $P < 0.01=**$) shown.

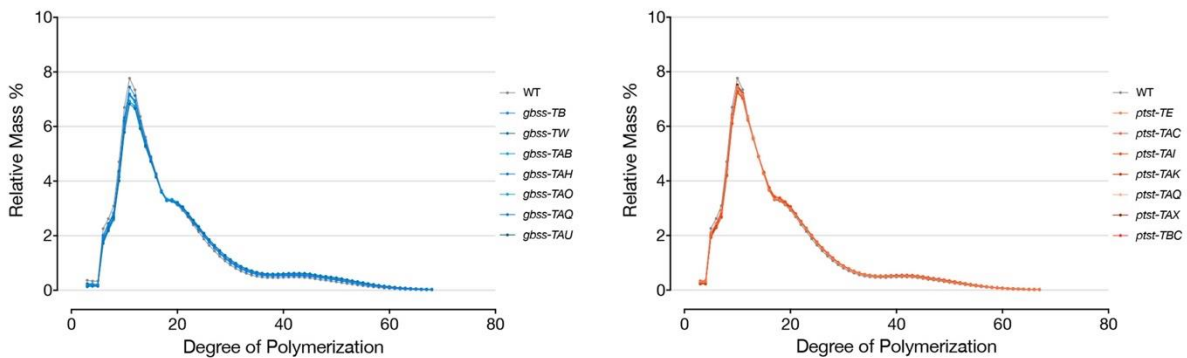


Fig. S5. CLDs in storage root starch of *gbss* and *ptst* lines. CLD was determined from *gbss* (left) and *ptst* (right) lines by analyzing debranched, purified starch granules. WT (grey line) is presented. Values represent the mean CLD determined. $n = 4$ plants, except *ptst*-TAQ $n = 3$ plants.

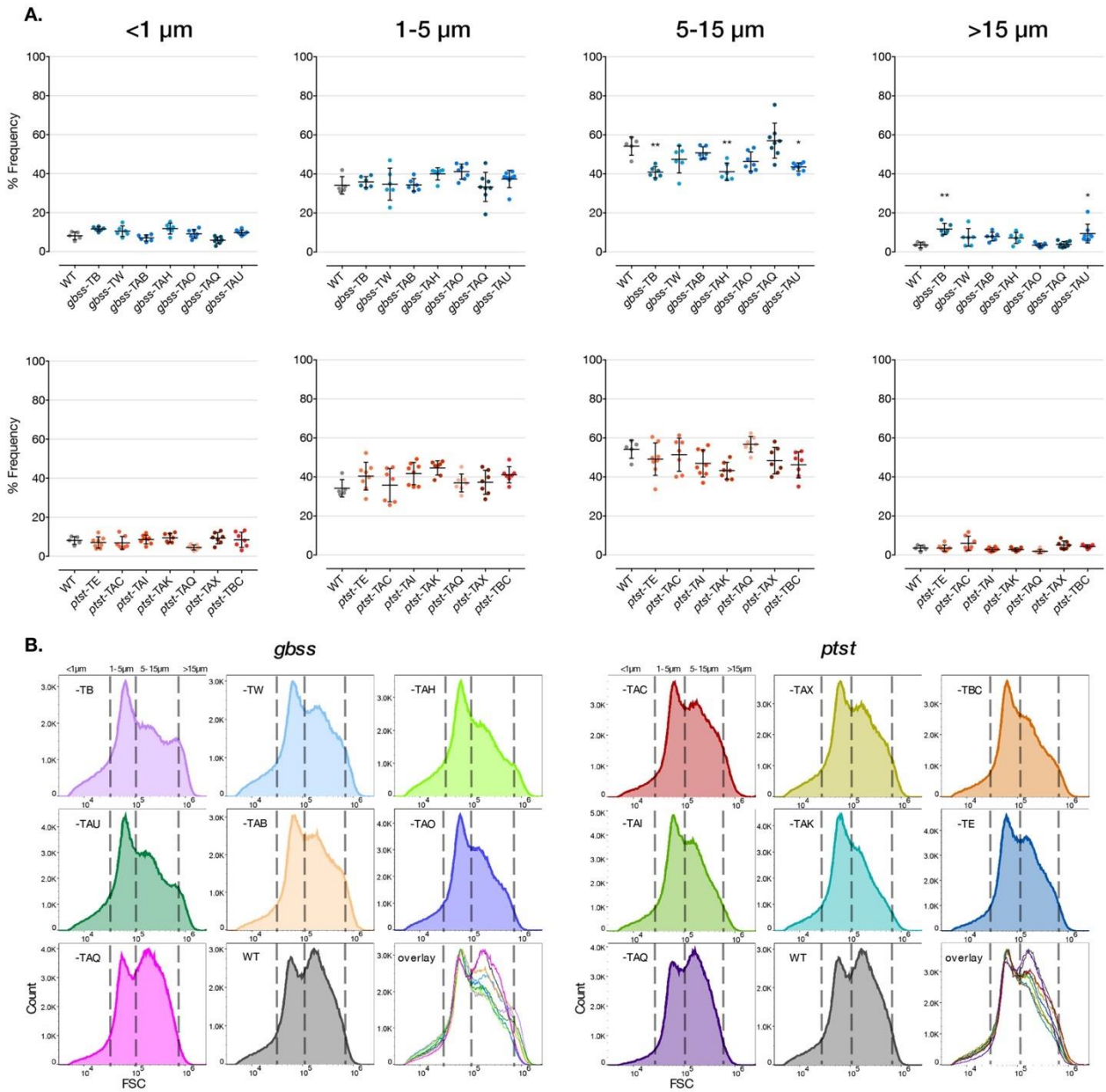


Fig. S6. Flow cytometry analysis of starch granule size in *gbss* and *ptst* lines. (A) Percentage

distribution of granule size from sample population (50,000 granules per sample) for *gbss* and *ptst* lines. Size categories were defined for *gbss* (upper graphs) and *ptst* (lower graphs).

Statistical analysis using Tukey's multiple comparisons test ($P < 0.01 = **$, $P < 0.05 = *$) are

shown. (B) Averaged distribution of granule size. Forward scatter (FSC). Size categories defined

as <1 μm, 1-5 μm, 5-15 μm and >15 μm. $n = 6-8$ plants.

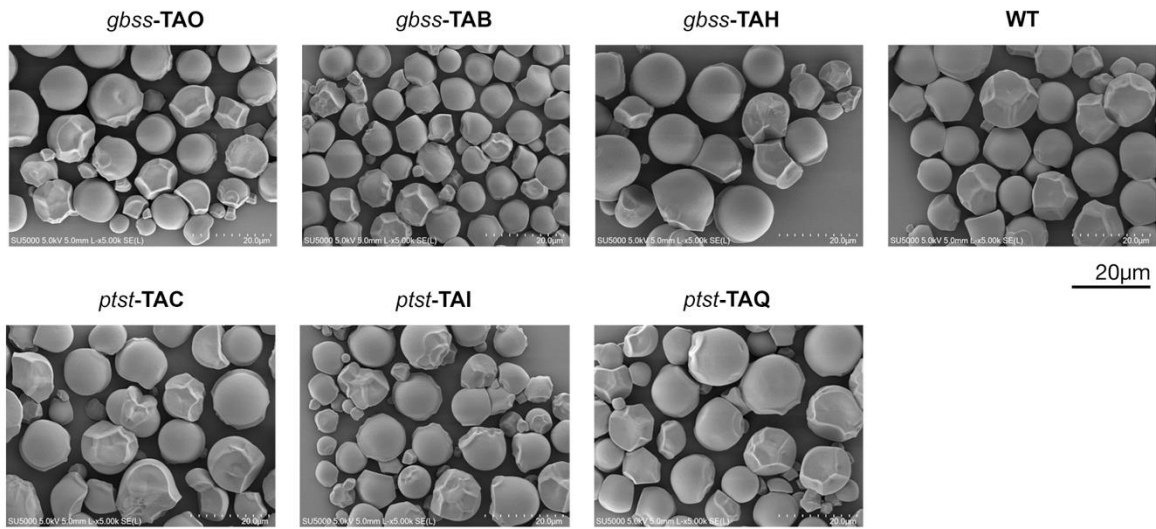


Fig. S7. Scanning electron microscopy of purified *gbss* and *ptst* starch granules. Purified starch from selected *gbss* (upper images) and *ptst* (lower images). WT also shown. Scale for all panels shown.

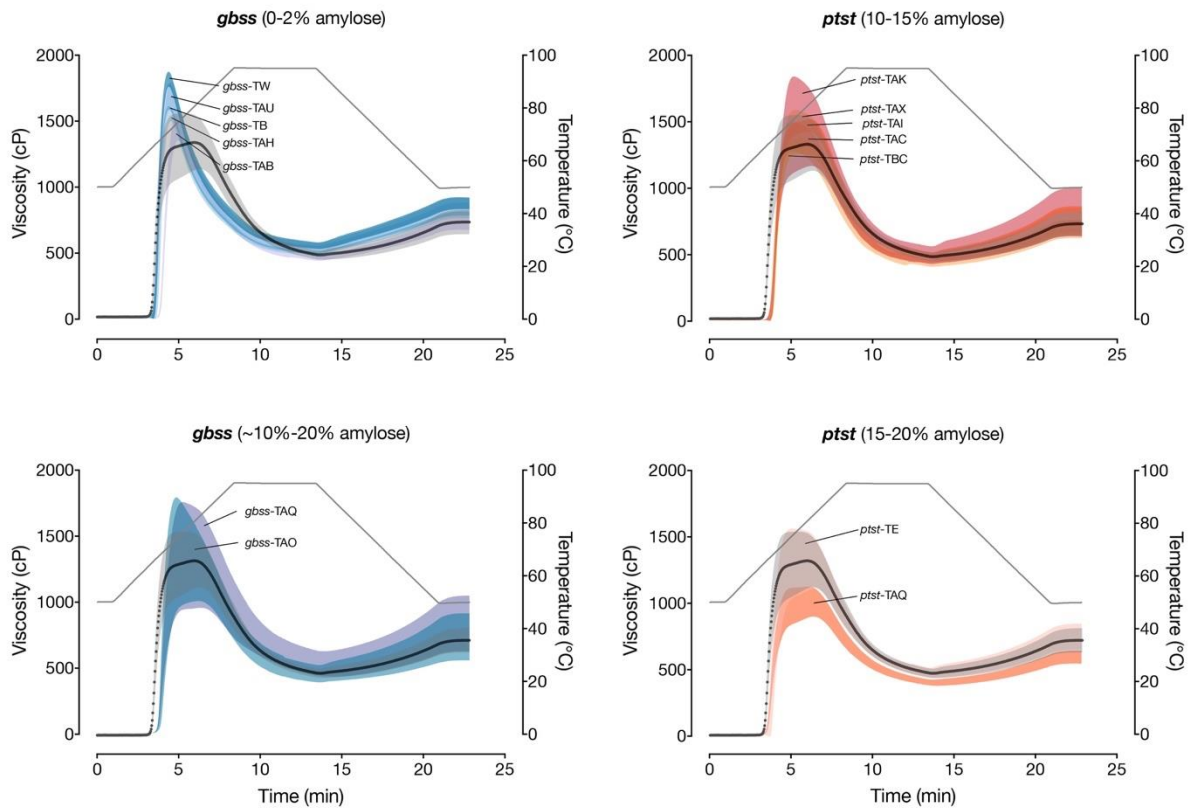


Fig. S8. Physicochemical properties of *gbss* and *ptst* starch. Viscosity measurements of purified starch from *gbss* and *ptst* lines. *gbss* lines (left) and *ptst* lines (right) separated based on ranges of amylose content. WT (black line, grey shading) overlaid on each graph for comparison. Temperature gradient is depicted as the grey line against the secondary (right) y-axis. Mean values ($n = 3-4$ plants, except *gbss*-TAQ and *ptst*-TBC, $n = 2$ plants) plotted with SD indicated by shading. Each line is labelled.